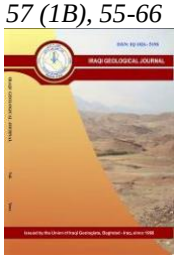
Iraqi Geological Journal

Journal homepage: https://www.igj-iraq.org



CBR Mapping Prediction from 2D Resistivity Imaging Using Regression Following Archie's Formula

Mohamed El Basri[1,] *, Hasnaa Harmouzi[2], Lahcen El Basri [3], Mohamed Mastere [1], Ibrahim Ouchen[1] Bouchta El Fellah[1] and Brahim Benzougagh[1]

[1] Department of Geomorphology and Geomatic, Scientific Institute, University Mohammed V in Rabat. Av. Ibn Batouta, B.P 703, 10106 Rabat, Morocco.
[2] Exploration and Geotechnics Team, Moulay Ismaïl University, FSM. B.P. 11201 Zitoune, Meknes, Morocco
[3] Department of Geology, Faculty of Sciences, University of Hassan II, Ain chock, Casablanca, Morocco
* **Correspondence**: mohamed.elbasri@is.um5.ac.ma

Received:
19 June 2023

Accepted:
31 October 2023

Published:
29 February 2024

Abstract

Indirect geophysical methods are increasingly associated with direct underground methods in investigating the subsurface to address environmental and geotechnical problems and reduce the cost of underground studies. These methods make it possible to explore large areas with acceptable precision, time, and cost. The present study combines the electrical resistivity method with the California Bearing Ratio for exploring an area located west of the Nouakchott port in Mauritania. The study aims firstly to verify that the thickness of the backfill layer must be less than 2 m throughout the entire study area and secondly to map areas with low California Bearing Ratio values (<80%) indicating substandard backfill compaction using 2D Electrical Resistivity Tomography imaging survey and regression. The measured Electrical Resistivity values exhibit a good nonlinear regression with California Bearing Ratio, following Archie's equation. A map of California Bearing Ratio variation was derived from the Electrical Resistivity values, indicating the distribution and variation of soil strength in the study area. The results revealed that the backfill layer did not meet the standards, with approximately 35% of the total area having a California Bearing Ratio value below 80%. The areas with poor compaction requiring treatment were primarily located in the southern sector, followed by the middle and eastern sectors.

Keywords: Resistivity; Tomography; Geotechnics; Map

1. Introduction

In the field of applied geology, geotechnical methods allow for accurate measurement of subsurface physical parameters, but the results are limited to the vicinity of the tested locations. Therefore, a large number of measurements are required to cover a large area with high resolution. On the other hand, geophysical methods enable faster acquisition of subsurface parameters along profiles that can cover long distances and greater depths. While they cannot replace drilling or testing, they are often a cost-effective and reliable way of imaging the subsurface to determine its properties (Anderson and Croxton, 2008). Consequently, geophysical methods are increasingly used as supplementary survey tools for subsurface soil investigation and as control surveys during the implementation and exploitation stages

DOI: 10.46717/igj.57.1B.5ms-2024-2-14

of projects (Agrahari et al., 2009; Marçal Sousa and César Gomes, 2020; Michael, 1995; Tong and Yang, 1990). Several previous studies have linked geophysical and geotechnical methods to investigate near-surface layers for various purposes (Abbas et al., 2022; Eissa, 2021; Jamiolkowski, 2012; Shahrabi et al., 2016). Asem and Gehan (2023) conducted a study on soil parameters such as grain size, moisture content, Atterberg limits, Standard Proctor SP, and Modified Proctor MP compaction tests of the same specimens. Their study revealed that resistivity is affected by and sensitive to key compaction parameters, namely moisture content, dry density, and compaction energy. They observed that, at low moisture content, increasing compaction effort leads to a sudden decrease in resistivity in a nonlinear manner. To construct the pavement in a specific area of the Nouakchott port, in Mauritania, a backfill layer was meticulously positioned and compacted. Mechanical energy was applied to the soil to rearrange its particles and reduce the void ratio, ultimately increasing its density. If this process is not carried out in accordance with the established standards, soil settlement can occur over time, resulting in avoidable maintenance expenses or even structural failure. Instead of relying on the SP or MP tests, the California Bearing Ratio (CBR) test (ASTM International, 2021) was utilized as a validation parameter to assess the compaction quality of this layer. The goal of this study is to generate a predicted map of CBR values for the study area based on measured and interpolated maps of electrical resistivity. This is achieved through an ER-CBR regression analysis following Archie's formula (Archie, 1942), which correlates porosity with water resistivity, soil resistivity, saturation and lithology (cementation factor). The primary objective is to establish a correlation between the measured ER of the soil and the corresponding CBR values. This correlation enables the mapping of sectors with CBR values below 80% using Electrical Resistivity Tomography (ERT) imaging. Additionally, the study involves monitoring the thickness of the initially compacted layer, ensuring it does not exceed 2 m.

2. Study Area and Local Lithology Sitting

The study area is situated in the Nouakchott port, west of the city, in Mauritania at coordinates 16°1'22" W, 17°59'44" N (Fig.1). This location is on the periphery of the expansive Senegalese-Mauritanian basin. The geological layers present in Nouakchott city and its immediate surroundings are primarily of Quaternary age, deposited over approximately one million years. These Quaternary formations consist of alternating marine shell deposits formed during transgressions and continental sediments formed during regressions (Caruba and Dars, 1991).

A local lithology assessment was conducted by drilling three boreholes to a depth of 15 meters (Fig.2 a). Analysis of the core samples retrieved from the boreholes reveals that the subsurface formations throughout the entire depth of investigation (15 meters) are predominantly composed of sand, with localized presence of shells. The uppermost layer consists of compacted artificially placed shelly sand, which overlies a thinner layer of coarse shelly sand. In the southern zone (borehole SC12), the thickness of this layer decreases, indicating lateral facies variation with clayey sand and shelly clayey sand observed in boreholes SC12 and SC10, respectively).

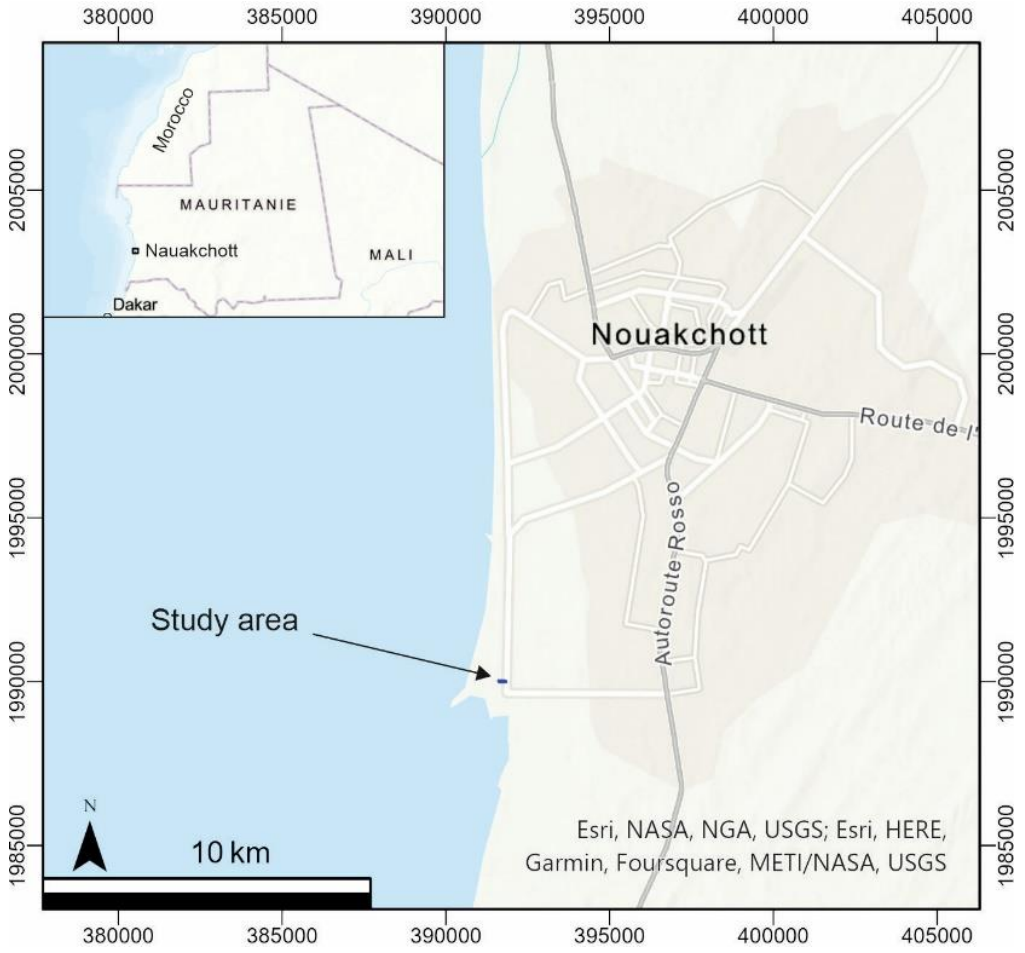


Fig.1. Study area location

3. Materials and Methods

3.1. The California Bearing Ratio (CBR)

The CBR is a test allowing to determine the bearing capacity of the subgrade constituted of particles with a maximum sizes less than 19 mm for road and airfield pavements (ASTM International, 2021). This test is applied to the surface and used in soil investigations as an aid to the design of pavements. It calculates the ratio of force per unit area required to penetrate a soil mass with a standard circular plunger of 50 mm diameter at the rate of 1.25 mm/min. The D 698 and D 1557 test methods determine the CBR of a material at optimum water content or range of water content from a specified compaction test and a specified dry unit weight (ASTM International, 2021). The water content and compaction (porosity) are factors influencing the electrical resistivity of a material (compacted or not). The relationship described by Archie's formula (Archie, 1942; Li et al., 2022) is given in Equation (1):

$$S_w = \sqrt[n]{\frac{abR_w}{R_t \emptyset^m}} \quad (1)$$

With:

S_w: water saturation, n: saturation exponent, a: tortuosity index (Winsauer et al., 1952), b: Rock wettability (Ransom, 1984), R_w: water resistivity, R_t: resistivity of partially saturated rock, $\emptyset$: porosity, m: cementation exponent.

The formula illustrates the relation between rock resistivity, water resistivity, water content and the porosity. The porosity of a soil is inversely proportional to its compaction, meaning a more compacted soil has lower porosity. Rock resistivity increases with compaction and decreases with water content. Hence, by measuring rock resistivity, we can estimate the CBR parameter.

CBR tests were conducted on artificially compacted subgrade layers in specific locations of the study area to assess the suitability for port pavement. In this case, a CBR threshold of greater than 80% is recommended to ensure adequate support for heavy traffic and the weight of trucks and machinery.

3.2. The Electrical Resistivity Tomography (ERT)

ERT was employed to visualize the spatial distribution of underground electrical resistivity along specific profiles. The data acquisition was conducted using the Lippmann 4-point light earth resistivity meter. The Wenner electrode configuration was utilized, employing 24 electrodes spaced at 4.5 meters intervals, enabling an investigation depth of up to 15 meters. A total of six ERT profiles were established, ensuring they passed through the same locations as the CBR test points for comprehensive analysis and correlation (Fig.2 b).

One of the crucial steps in any geophysical prospection is to determine the physical model that best represents the subsurface geology, ensuring a close fit to the observed data. This is achieved through various data inversion methods and approaches, each offering reliable results based on the available a priori information. Some commonly used methods include smoothness constrained, Occam's, Marquardt, focused, polygonal, and layered media (Constable et al., 1987; Marquardt, 1963; Pinheiro et al., 1997; Portniaguine and Zhdanov, 1999).

The drilling company provided essential a priori information (Fig.2**Error! Reference source not found.**), including the layer thicknesses at specific locations, indicating a layered subsurface. The inversion process for all ERT data profiles was performed using the Zondres2D software version 7, utilizing both smoothness constrained and Occam's inversions.

In this particular study, special attention was given to monitoring the thickness of the artificially compacted layer, also known as the backfill layer. It was essential to ensure that the thickness did not exceed 2 meters, as per the specific requirement of the customer. This limitation was imposed throughout the entire study area to maintain consistency and adherence to the project specifications.

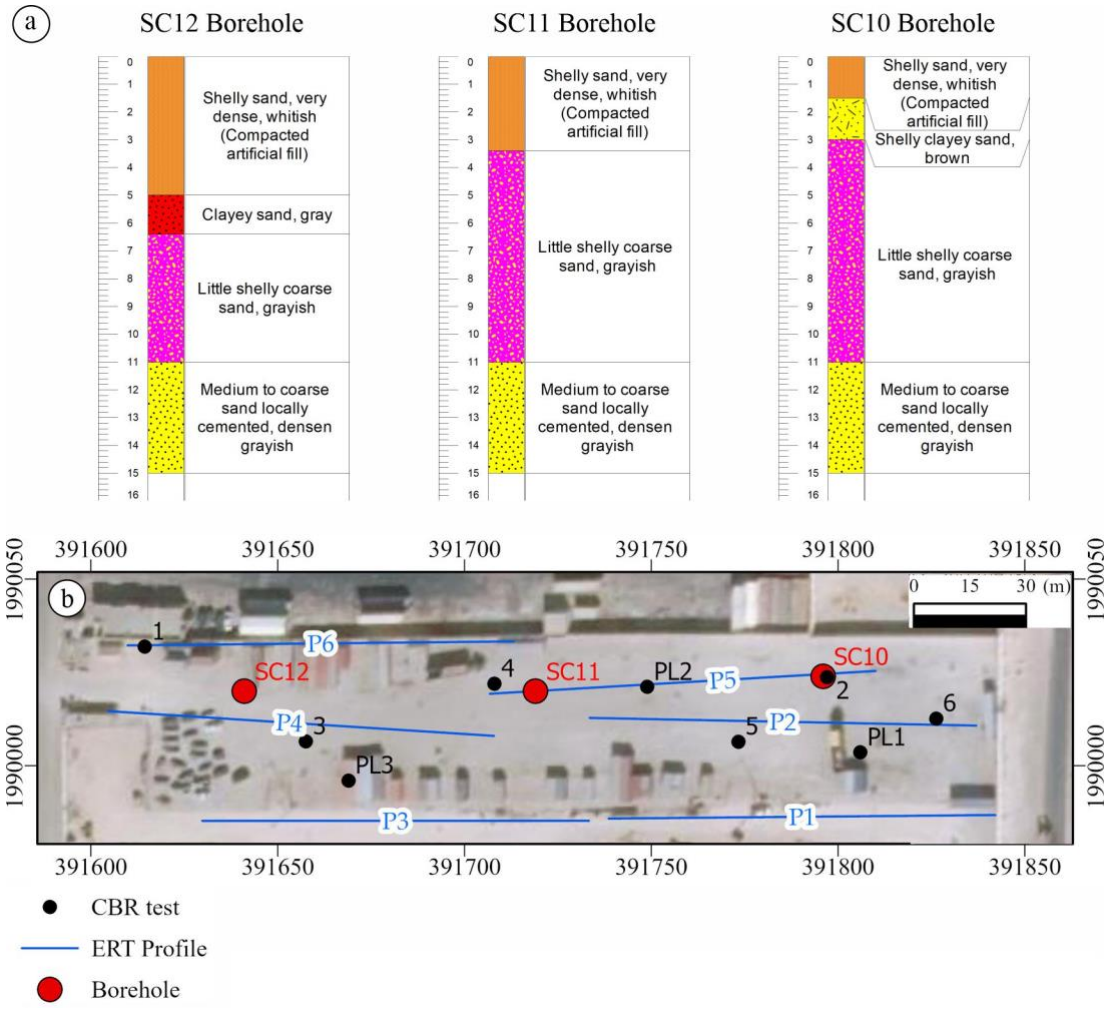


Fig.2. (a) Borehole's lithology; (b) Borehole, CBR test and ERT profile's locations.

3.3. CBR vs Resistivity Correlation

To interpret the results, it was assumed that the water content (saturation) and water resistivity of the artificially compacted backfill layer remained constant. As a result, based on the Archie equation (1), only the porosity $\emptyset$ varies with the artificial compaction. The relationship between compaction and porosity can be described as follows:

$$C = 1 - \emptyset \tag{2}$$

These equations (1) and (2) can be utilized to establish the following relationship:

$$R_t = \frac{abR_w}{S_w^2\ (1-C)^m} \tag{3}$$

Depending on this equation the resistivity R_t increase when the compaction C increase.

The compaction C is then:

$$S_w^2\ (1-C)^m\ = \frac{abR_w}{R_t} \tag{4}$$

$$(1-C)^m\ = \frac{abR_w}{S_w^2 R_t} \tag{5}$$

$$(1 - C) = \sqrt[m]{\frac{abR_w}{S_w^2 R_t}} \quad (6)$$

$$C = 1 - \sqrt[m]{\frac{abR_w}{S_w^2 R_t}} \quad (7)$$

The compaction C is a function of the CBR:

$$C = f(CBR) \quad (8)$$

To simplify, it is assumed that C is a simple linear function of CBR:

$$C = k.CBR \quad (9)$$

Where k is a constant cofficient.

From equations (7) and (9), it follows that:

$$CBR = \left[1 - \sqrt[m]{\frac{aR_w}{S_w^n R_t}}\right] \times \frac{100}{k} \quad (10)$$

The multiplication by 100 is used because CBR is measured in percentage.

4. Results and Discussion

4.1. California Bearing Ratio (CBR) Test

A total of ten CBR tests were conducted in the vicinity of the study area (Fig.2 b, Table 1). To expand the dataset, three additional values were calculated using the LCPC formula (LCPC-SETRA, 1994) (PL1, PL2, PL3; Table 1). The CBR values obtained from all the tests ranged between 72% and 100%. It is recommended that the CBR value for adequate compaction should be equal or greater than 80%.

Table 1. CBR tests results.

Points	X (m)	Y (m)	CBR (%)	Resistivity (Ohm.m)
1	391625	1990027	93	254.0
2	391635	1990036	100	350.0
3	391666	1990006	72	49.8
4	391708	1990022	100	265.1
5	391736	1990032	91	208.3
6	391776	1990006	90	185.4
7	391793	1990021	100	255.0
8	391790	1990036	100	317.0
9	391826	1990016	85	148.9
10	391837	1990022	78	65.5
PL1	391821	1990001	88	109.5
PL2	391752	1990028	100	255.8
PL3	391669	1989998	74	55.6

4.2. Electrical Resistivity Tomography (ERT) Profiles

The ERT profiles were arranged in a west-to-east direction, comprising three profiles located to the west and three profiles to the east of the study area (Fig.2). These profiles were strategically plotted to intersect boreholes and CBR test locations, ensuring comprehensive coverage across the entire study area. Among these profiles, the first inverted profile was P5, as it traversed the SC11 and SC10 boreholes, which provided valuable preliminary information about the thicknesses of geological layers and the water table level.

To enhance the accuracy of the data, several adjustments were made. Firstly, to improve the forward modeling of significant resistivity differences near the surface, that can cause significant distortions in the lower sections of the inversion model; a model cells with widths of half the unit spacing was used (Loke, 2004). Secondly, data points exhibiting substantial misfit errors were removed from the analysis. As a result of these refinements, the root mean square (RMS) of all profiles was determined to be less than 10%.

The resistivity within the vicinity of the study area, extending from the surface to a depth of 15 meters, exhibits a range of values from 1 Ohm.m to 350 Ohm.m (Fig.3). Generally, the underground of the area can be divided, from top to bottom, into four electrical horizons or layers, and each characterized by an average resistivity: 220 Ohm.m, 40 Ohm.m, 20 Ohm.m, and 7 Ohm.m. To establish a correlation between these electrical horizons and the lithostratigraphy observed in the boreholes, analysis was conducted specifically on profile P5 (Fig. 2 and 3).

The first layer, a compacted section consisting of dense whitish shelly sand, has varying thicknesses at the SC11 and SC10 boreholes, measuring 3.2 meters and 1.3 meters respectively. Within this layer, the resistivity values range from 100 Ohm.m to 300 Ohm.m, with a predominant value of 290 Ohm.m. Notably, two anomalies of low resistivity are observed at distances of 25 meters and 35 meters. These anomalies can be attributed to differences in compaction levels, as all other factors remain constant and the layer itself consists of the same material with a consistent water content.

Below this layer, the borehole data reveals lateral variations in facies. Towards the western side of the profile (borehole SC11), the layer overlays a small section of shelly coarse sand, while on the eastern side (borehole SC10), it overlays shelly clayey sand. At the borehole level, this layer takes the form of a depression zone, and this pattern repeats at three locations along the profile, approximately at distances of 20 meters, 33 meters and 66 meters. This suggests the possible extension of this layer in other profiles.

This second layer exhibits a resistivity contrast between its western side (7 Ohm.m) and eastern side (20 Ohm.m). Since the groundwater in the area is influenced by saltwater intrusion from the ocean along the coastal strip, the water table depth ranges from 2 to 4 meters (DATAR, 2000). This resistivity contrast may be attributed to the presence of clay within the formation, which affects its porosity and subsequently the saline water content. The varying resistivity values are indicative of the fluctuating amount of saline water present in the formation.

Negative resistivity anomalies are predominantly observed in the middle and northern sections of the study area, specifically in profiles P4, P2, P6, and P5. Conversely, the southern part of the study area, represented by profiles P3 and P1, exhibits a lower resistivity contrast.

The thickness of the first artificially compacted layer displays variations across different profiles. For instance, in profile P4, at a distance 20 meters, the thickness exceeds 3 meters. On the other hand, profile P6 showcases locations where the thickness is less than 2 meters.

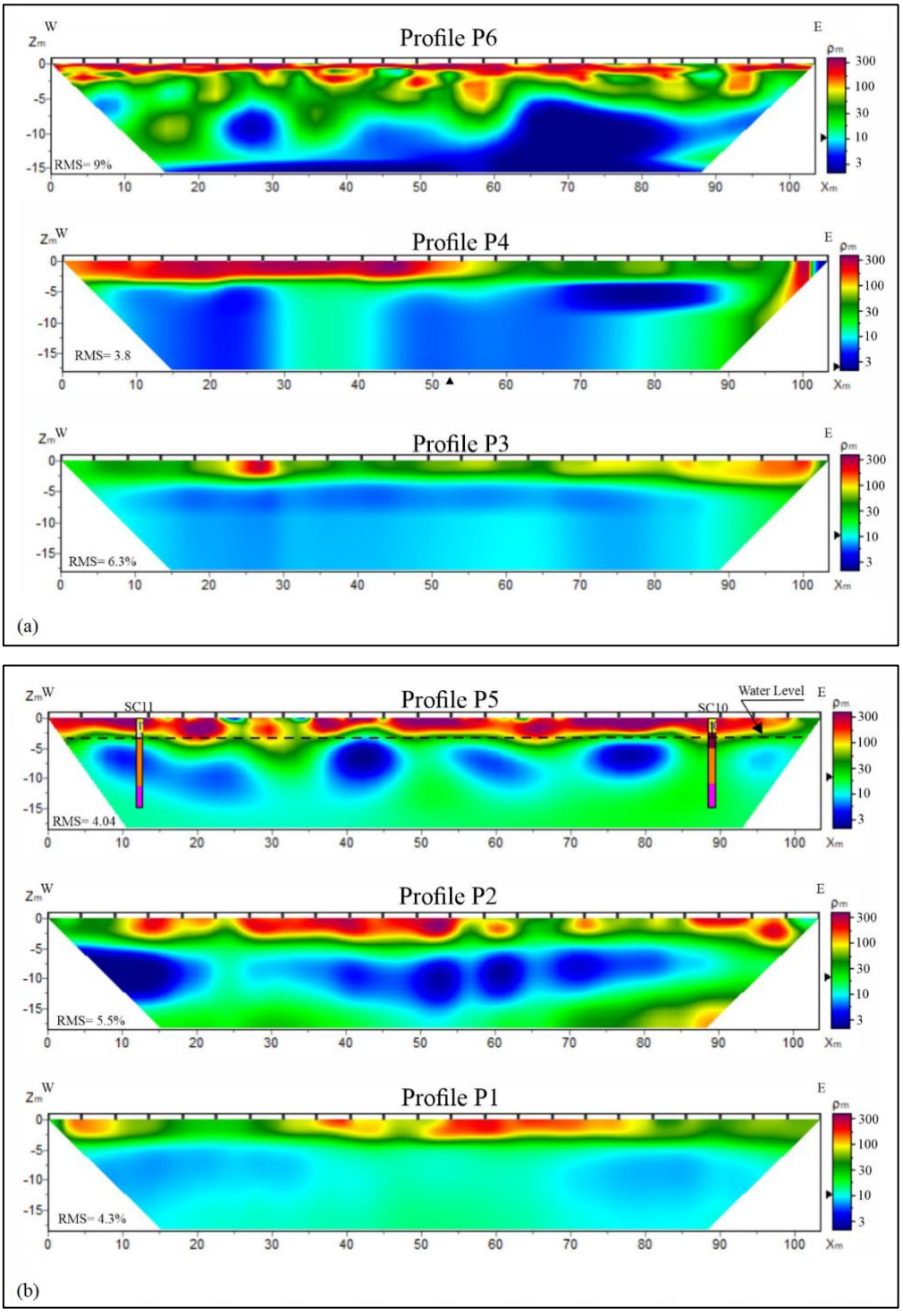


Fig.3. ERT profiles of the western (a) and the eastern (b) zones of the study area. And boreholes data used for inversion of profile P5 (the water level (WL) is between 2.3 to 3 m depth).

4.3. Resistivity Map

The resistivity map was generated by interpolating resistivity values extracted from the exported mesh model of all profiles. Specifically, values within the depth range of 0 to 0.3 meters were selected as representative resistivity values for the compacted artificial layer (Fig. 4a). This map illustrates lateral

variations in resistivity, with relatively high resistivity observed in the northern part and low resistivity in the southern part of the study area.

Furthermore, the resistivity shows an increasing trend from the south to the north, and repetitive fluctuations are observed when moving from east to west. These variations in resistivity can be attributed to differences in the degree of artificial compaction, as the same material was used for backfilling throughout the area. Figure 4a provides a qualitative representation of the variation in compaction levels.

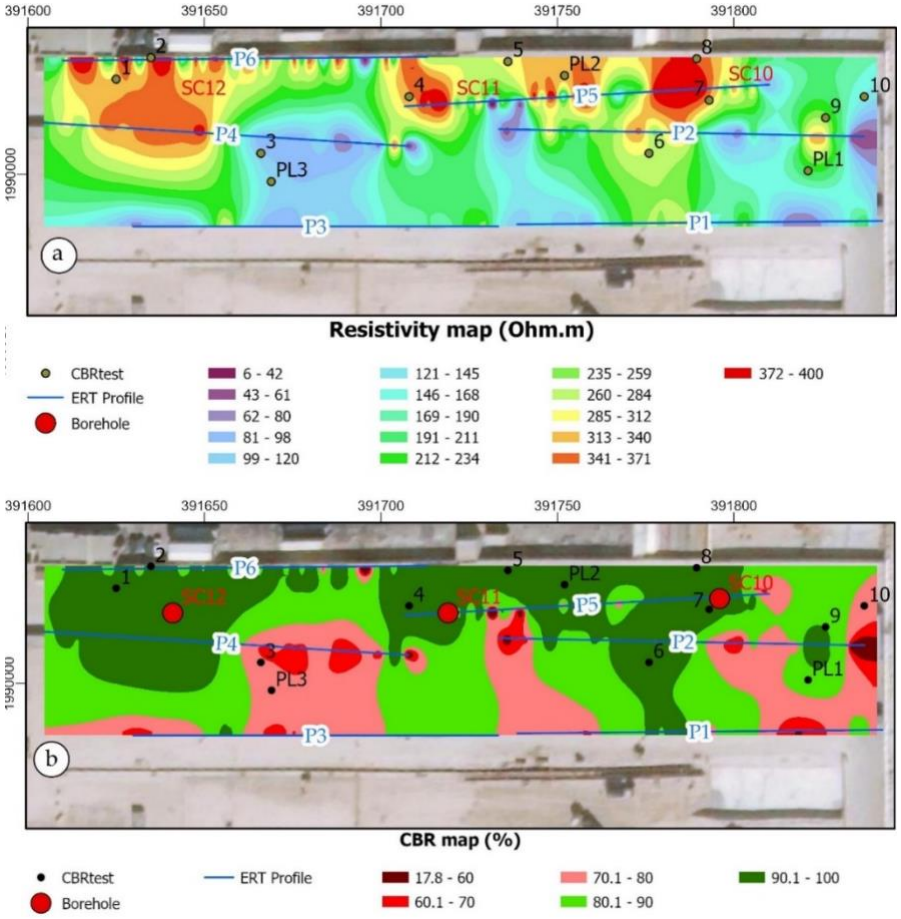


Fig.4. (a) resistivity map; (b) CBR regression map following equation (12).

4.4. CBR and Resistivity Regression

To establish a regression formula linking the CBR value to the resistivity (Rt) of the formation, the "Curve Fitting Tool" in MATLAB software was employed. The equation (10) provided in the literature served as the basis for this regression analysis, which establishes the relationship between CBR and resistivity.

Using the interval variations of all parameters listed in Table 2, which were derived from the relevant literature (Table 3), the Curve Fitting Tool facilitated a nonlinear least squares optimization. This optimization employed the Trust-Region Algorithm (Coleman and Li, 1996; Moré and Sorensen, 1983) to predict all the coefficients of equation (10).

Figure 5 depicts the curve fitting results, illustrating the relationship between CBR and resistivity. Moreover, the predicted coefficients, along with their 95% confidence bounds, are presented in the accompanying table. This regression analysis provides a formula that can estimate the CBR value based

on the resistivity (Rt) of the formation, taking into account the interval variations of the parameters from Table 2, as derived from the literature (Table 3).

Finally, the equation giving the relation between CBR and R_t.is given by:

$$CBR = \left[1 - \sqrt[4.065]{\frac{0.3768 * 1.209}{0.3405^{1.8} * R_t}}\right] \times \frac{100}{0.6833} \quad (11)$$

$$CBR = \left[1 - \sqrt[4.065]{\frac{3.17}{R_t}}\right] \times 146.35 \quad (12)$$

The water resistivity (Rw = 1.209 Ohm.m) is relatively low due to the utilization of saltwater from boreholes (DATAR, 2000) during the preparation of the artificial compacted layer. Other parameters fall within the range defined by the lower and upper limits as provided in Table 3. The value of (m) is close to the upper limit proposed by Rivero (1977) for sandstones, while the value of (a) is near the lower limit suggested by Hill and Milburn (1956).

Using the resistivity map (Fig. 4a), we calculated the predicted CBR map based on equation (12). The resulting CBR map is shown in Figure 4b, where green areas indicate CBR values above 80% and red areas indicate CBR values below 80%. Regions with poor compaction, requiring treatment, are primarily located in the southern, middle, and eastern sectors.

Table 2. The start values, lower limits, and upper limits used in the nonlinear least squares regression for equation (10), along with their predicted values and 95% confidence bounds, are presented below. The lower and upper limits were chosen based on the minimum and maximum ranges provided in Table 3.

Coefficients	Start Point	Lower limit	Upper limit	Regression coefficient (with 95% confidence bounds)
a	0.63	0.004	17.7	0.3768
k	0.2	0.1	1	0.6833
m	1	0.02	5.67	4.065
n	1.8	1.8	3	1.8
R_w	2	0.01	20	1.209
S_w	0.3	0.1	0.4	0.3405

Table 3. Ranges of Archie exponent a and coefficient m (Worthington, 1993)

Lithology	A	M	Investigator (s)
Sandstones	0.47-1.8	1.64-2.23	(Hill and Milburn, 1956)
	0.62-1.65	1.3-2.15	(Carothers, 1968)
	1.0-4.0	0.57-1.85	(Porter and Carothers, 1970)
	0.48-4.31	1.2-2.21	(Timur et al., 1972)
	0.0004-17.7	0.02-5.67	(Rivero, 1977)
Carbonates	0.73-2.3	1.64-2.10	(Hill and Milburn, 1956)
	0.45-1.25	1.78-2.38	(Carothers, 1968)
	0.33-78.0	0.39-2.63	(Rivero, 1977)
	0.35-0.8	1.7-2.3	(Schön, 1983)

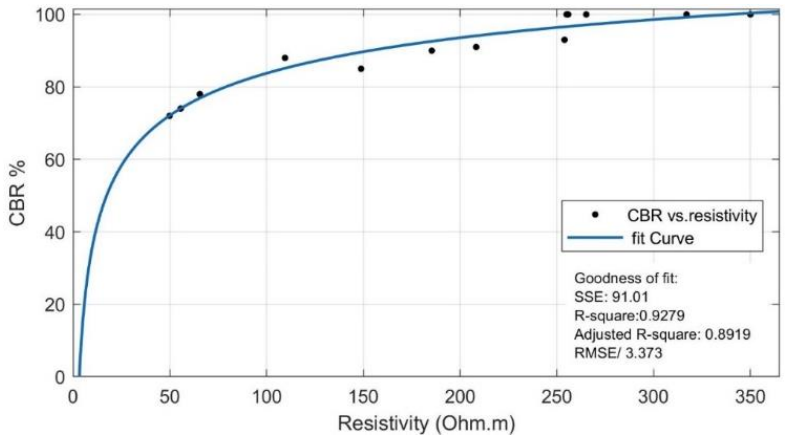


Fig.5. Regression of CBR vs Resistivity.

5. Conclusions

Inadequate soil compaction can have severe consequences, including significant structural distress, excessive total settlement, and differential settlement. It can result in the cracking of pavements, soils, and basements, as well as cause damage to buried structures, water and sewer lines, and utility lines. Furthermore, improper soil compaction can contribute to erosion and present environmental challenges.

The calculated CBR map highlights several areas within the study area where the CBR values are below 80%. These regions, primarily located in the southern, eastern, and central parts, indicate that the construction of the backfill layer did not meet the required standards. Therefore, appropriate treatment is essential to ensure adequate soil compaction and mitigate potential structural damage and environmental issues. The thickness of the backfill layer ranges from 0.8 meters to 4 meters. Notably, the weakest values are observed in the northwest (profile P6), where the thickness falls below 2 meters. In all other zones, the thickness ranges between 2.5 meters and 4 m. This study underscores the significance of geophysical data, specifically ERT, in accurately mapping subsurface layers and estimating the CBR of an artificial layer in a cost-effective manner. Regression analysis, utilizing Archie's equation, demonstrated a strong fit with an R-square value of 0.9279. All parameters derived from this equation fall within the suggested limits for sandstones, as proposed by previous researchers.

Acknowledgements

The authors are very grateful to the Polygeo company and extend heartfelt appreciation and special thanks to Mr. Lahcen El Basri, and all my colleagues who helped us.

6. References

Abbas, S.S., Ahmed, M.M., Abed, A.M., 2022. Determination of civil engineering problems using resistivity methods in Ramadi, Western Iraq. Iraqi Geological Journal 55, 160–165.

Agrahari, S., Israil, M., Mittal, S., Rai, J., 2009. Soil characterization using electrical resistivity tomography and geotechnical investigations. Journal of Applied Geophysics 67, 74–79.

Anderson, N., Croxton, N., 2008. Geophysical methods commonly employed for geotechnical site characterization, July 2008. ed, Transportation research circular. Transportation Research Board 500 Fifth Sreet, NW Washington, DC 20001, Washington.

Archie, G.E., 1942. The electrical resistivity log as an aid in determining some reservoir characteristics. Transactions of the AIME 146, 54–62.

Asem A, H., Gehan U, N., 2023. Geotechnical-electrical evaluation of soil compaction parameters, south of Baqubah city. Iraqi Geological Journal, 56, 144–155.

ASTM International, 2021. Standard test method for california bearing ratio (CBR) of laboratory-compacted soils, D1883-21st ed. ASTM International.

Carothers, J., 1968. A statistical study of the formation factor relation to porosity: The Log Analyst, 9(5) 13–20.

Caruba, R., Dars, R., 1991. Géologie de la Mauritanie. Mauritanie.

Coleman, T.F., Li, Y., 1996. An interior trust region approach for nonlinear minimization subject to bounds. SIAM Journal on Optimization 6, 418-445.

Constable, S.C., Parker, R.L., Constable, C.G., 1987. Occam's inversion: A practical algorithm for generating smooth models from electromagnetic sounding data. Geophysics 52, 289–300.

DATAR, 2000. Plan d'aménagement du littoral mauritanien (No. Phase 1).

Eissa, R., 2021. Electrical resistivity tomography application for buried foundation Investigations: Insights and review. Iraqi Geological Journal, 54, 122–133.

Hill, H., Milburn, J., 1956. Effect of clay and water salinity on eletrochemical behavior of reservoir rocks. Petroleum Transactions, 207.

Jamiolkowski, M., 2012. Role of geophysical testing in geotechnical site characterization. Soils and Rocks 35, 117–137.

LCPC-SETRA, 1994. Conception et dimensionnement des structures de chaussée.

Li, Y., Liu, X., Cai, C., Hu, Z., Wu, B., Mu, Y., Duan, X., Zhang, Q., Zeng, S., Guo, J., Pu, Z., 2022. A laboratory approach considering salinity to investigate archie's parameters in deep shale: A case study in Longmaxi formation, southern Sichuan. Geofluids 2022, 1-15.

Loke, M.H., 2004. Tutorial: 2-d and 3-d electrical imaging surveys.

Marçal Sousa, G., César Gomes, R., 2020. Obtaining geotechnical parameters from correlations between geophysics and CPT tests in tailings dams. REM - International Engineering Journal, 73, 453–462.

Marquardt, D.W., 1963. An algorithm for least-squares estimation of nonlinear parameters. Journal of the Society for Industrial and Applied Mathematics, 11, 431–441.

Michael, P., 1995. A geophysical site investigation for a bridge foundation in a narrow Canyon. International Journal of Rock Mechanics and Mining Sciences and Geomechanics Abstracts 1, 1219–1226.

Moré, J.J., Sorensen, D.C., 1983. Computing a trust region step. Siam Journal on Scientific and Statistical Computing, 4, 553–572.

Pinheiro, P.A.T., Loh, W.W., Dickin, F.J., 1997. Smoothness-constrained inversion for two-dimensional electrical resistance tomography. Measurement Science and Technology 8, 293.

Porter, C.R., Carothers, J.E., 1970. Formation factor-porosity relation derived from well log data, in: SPWLA 11th Annual Logging Symposium. OnePetro.

Portniaguine, O., Zhdanov, M.S., 1999. Focusing geophysical inversion images. Geophysics 64, 874–887.

Ransom, P.C., 1984. A contribution toward a better understanding of the modified archie formation resistivity factor relationship. The Log Analyst, 25.

Rivero, O.G., 1977. Some considerations about the possible use of the parameters a and m as a formation evaluation tool through well logs, in: SPWLA 18th Annual Logging Symposium. OnePetro.

Schön, J., 1983. Petrophysik.

Shahrabi, M.M., Jafarzadeh, F., Akbari Garakani, A., Eskandari, N., Banikheir, M., Farahi, H., 2016. Comparison of liquefaction evaluation based on SPT and geophysical tests (case study: Mahabad dam, Iran). Presented at the International Conference Geotechnical and Geophysical Site Characterization, Queensland.

Timur, A., Hempkins, W., Worthington, A., 1972. Porosity and pressure dependence of formation resistivity factor for sandstones, in: Trans CWLS 4th Formation Evaluation Symp.

Tong, L.T., Yang, C. H., 1990. Incorporation of topography into two-dimensional resistivity inversion. GEOPHYSICS 55, 354–361.

Winsauer, W.O., Shearin, H.M., Jr., Masson, P.H., Williams, M., 1952. Resistivity of Brine-Saturated Sands in Relation to Pore Geometry1. AAPG Bulletin 36, 253–277.

Worthington, P., 1993. The uses and abuses of the archie equations, 1: The Formation Factor-Porosity Relationship. Journal of Applied Geophysics, 30, 215–228.